A new type of radiosensitive T⁻B⁻NK⁺ severe combined immunodeficiency caused by a *LIG4* mutation

Mirjam van der Burg,[1] Lieneke R. van Veelen,[2,3] Nicole S. Verkaik,[2] Wouter W. Wiegant,[4] Nico G. Hartwig,[5] Barbara H. Barendregt,[1,5] Linda Brugmans,[2] Anja Raams,[2] Nicolaas G.J. Jaspers,[2] Malgorzata Z. Zdzienicka,[4,6] Jacques J.M. van Dongen,[1] and Dik C. van Gent[2]

[1]Department of Immunology and [2]Department of Cell Biology and Genetics, Erasmus Medical Center, Rotterdam, The Netherlands. [3]Department of Radiation Oncology, Erasmus Medical Center–Daniel den Hoed Cancer Center, Rotterdam, The Netherlands. [4]Department of Toxicogenetics, Leiden University Medical Center, Leiden, The Netherlands. [5]Department of Pediatrics, Division of Immunology and Infectious Diseases, Erasmus Medical Center–Sophia Children's Hospital, Rotterdam, The Netherlands. [6]Department of Molecular Cell Genetics, Collegium Medicum, Nicolaus Copernicus University, Bydgoszcz, Poland.

V(D)J recombination of Ig and TCR loci is a stepwise process during which site-specific DNA double-strand breaks (DSBs) are made by RAG1/RAG2, followed by DSB repair by nonhomologous end joining. Defects in V(D)J recombination result in SCID characterized by absence of mature B and T cells. A subset of T⁻B⁻NK⁺ SCID patients is sensitive to ionizing radiation, and the majority of these patients have mutations in Artemis. We present a patient with a new type of radiosensitive T⁻B⁻NK⁺ SCID with a defect in DNA ligase IV (LIG4). To date, LIG4 mutations have only been described in a radiosensitive leukemia patient and in 4 patients with a designated LIG4 syndrome, which is associated with chromosomal instability, pancytopenia, and developmental and growth delay. The patient described here shows that a LIG4 mutation can also cause T⁻B⁻NK⁺ SCID without developmental defects. The LIG4-deficient SCID patient had an incomplete but severe block in precursor B cell differentiation, resulting in extremely low levels of blood B cells. The residual D_H-J_H junctions showed extensive nucleotide deletions, apparently caused by prolonged exonuclease activity during the delayed D_H-J_H ligation process. In conclusion, different LIG4 mutations can result in either a developmental defect with minor immunological abnormalities or a SCID picture with normal development.

Introduction

During B and T cell differentiation, the Ig and TCR genes undergo V(D)J recombination in order to generate antigen-specific receptors (1, 2). This process is initiated through induction of DNA double-strand breaks (DSBs) by the recombination-activating gene 1 (RAG1) and RAG2 proteins between the coding V (D) and J elements and their flanking recombination signal sequences (RSSs) (3, 4). The resulting signal ends of both RSSs can directly be ligated into a signal joint, whereas the coding ends are covalently sealed hairpins, which require further processing prior to coding joint formation. The initiation of V(D)J recombination is lymphoid specific, but recognition and repair of the generated DNA ends occur via the general nonhomologous end joining (NHEJ) pathway of DNA DSB repair (5). During the processing phase of the coding ends, nucleotides can be lost because of exonuclease activity, and nontemplated (N) nucleotides can be introduced by terminal deoxynucleotidyl transferase (TdT) (6, 7).

DSBs are not only generated during V(D)J recombination but can also be induced by ionizing radiation (IR), reactive oxygen species, or certain drugs (8). In most mammalian cells, NHEJ is the major DSB repair pathway. In the initial phase of NHEJ, DSBs are recognized by the DNA-dependent protein kinase (DNA-PK) complex, which is composed of the DNA-PK catalytic subunit (DNA-PKcs) and the KU70/KU80 heterodimer that directly binds the DNA ends (9). The DNA-PK complex is a nuclear serine/threonine protein kinase that is activated upon association with DNA ends (9, 10). The Artemis protein can be phosphorylated by DNA-PK and is involved in opening of hairpin-sealed coding ends in V(D)J recombination (11, 12). In the final phase of NHEJ, the DNA ligase IV/XRCC4 (LIG4/XRCC4) complex catalyzes the ligation step (1, 8, 13).

Defects in V(D)J recombination result in SCID characterized by absence of mature B and T cells, but presence of NK cells. In 20–30% of these patients, mutations are found in the *RAG1* and *RAG2* genes (14). A subset of the remaining patients shows hypersensitivity to IR, suggesting a defect in NHEJ (15). A large fraction of these patients have mutations in the *Artemis* gene (11, 16–19). Patients with hypomorphic mutations in the *Artemis* gene have polyclonal B and T cell populations and a predisposition for lymphoma development (20). Recently, Dai et al. reported a radiosensitive (RS) SCID patient without mutations in any of the known NHEJ factors, suggesting that an additional factor is required for NHEJ and V(D)J recombination (21).

In the components of the DNA-PK complex, no defects have been found in humans. From the phenotypes of knockout mice it is known that *DNA-PKcs* defects lead to an RS-SCID phenotype with a predisposition to develop T cell tumors. *KU70* and *KU80* knockout mice show growth retardation, in addition to the RS-SCID phenotype (8). *LIG4* and *XRCC4* knockout mice die pre-

Nonstandard abbreviations used: DNA-PK, DNA-dependent protein kinase; DNA-PKcs, DNA-PK catalytic subunit; DSB, double-strand break; IR, ionizing radiation; IRIF, IR-induced foci; Kde, κ-deleting element; N, nontemplated; NBS, Nijmegen breakage syndrome; NHEJ, nonhomologous end joining; P, palindromic; RAG, recombination-activating gene; RS, radiosensitive; RSS, recombination signal sequence; TdT, terminal deoxynucleotidyl transferase.

Conflict of interest: The authors have declared that no conflict of interest exists.

Citation for this article: *J. Clin. Invest.* **116**:137–145 (2006). doi:10.1172/JCI26121.

Table 1
Absolute numbers of B, T, and NK cells in peripheral blood and percentages of precursor B cells and mature CD22+ B cells in BM of patient SC2 compared with RAG-deficient and Artemis-deficient SCID patients and healthy controls

	Patient SC2	RAG-deficient SCID	Artemis-deficient SCID	Healthy controls (9–15 mo)
Peripheral blood		*n* = 3	*n* = 3	*n* = 70[A]
B cells (× 10^9/l)	0.01	0.001	0.001	0.6–2.7
T cells (× 10^9/l)[B]	0.23	0.20	0.51	1.6–6.7
NK cells (× 10^9/l)	0.5	1.12	1.11	0.2–1.2
BM		*n* = 7	*n* = 4	*n* = 6
% Precursor CD22+ B[C]	11	32 ± 24	17 ± 14	31 ± 10
% Mature CD22+ B[D]	0.1	0.009 ± 0.01	0.004 ± 0.003	19 ± 5

[A]See ref. 49. [B]T cells of SCID patients can be autologous or maternal (50). T cells of patient SC2 were autologous. [C]The percentage of precursor B cells was calculated by subtraction of the percentage of mature SmIgM+SmIgD+ B cells from the total percentage of CD22+ B cells within the flow cytometric lymphogate (16, 44, 51). [D]Within the flow cytometric lymphogate.

natally because of apoptosis of postmitotic neurons (18, 22–24). The neuronal defect of *LIG4*- or *XRCC4*-deficient mice can be rescued by a homozygous mutation in *TP53* or *ATM* (25–27). However, the V(D)J recombination process cannot be rescued, and pro-B cell lymphomas develop soon after birth. To date, mutations in *XRCC4* have not been found in humans, whereas the mutations in *LIG4* that have been reported resulted in radiosensitivity and leukemia in 1 patient (28) and in pancytopenia and developmental and growth delay, collectively called the LIG4 syndrome, in 4 other patients (19, 29). Recently, another patient was described with a homozygous *LIG4* mutation, who presented with acute T cell leukemia and had a facial gestalt strongly reminiscent of Nijmegen breakage syndrome (NBS) (30). In this paper, we present a patient with a new type of RS-SCID with a mutation in *LIG4*, who presented not with developmental and growth delay characteristics of the LIG4 syndrome, but with a clinical SCID picture due to strongly affected V(D)J recombination.

Results

Patient with a new type of T–B–NK+ SCID. Patient SC2 was clinically and immunologically diagnosed with T–B–NK+ SCID (see "*Case report*" below). No developmental defects, growth delay, or microcephaly were observed. Flow cytometric analysis of peripheral blood showed a strong reduction of the absolute numbers of CD19+ B cells and CD3+ T cells, but normal absolute numbers of NK cells fully comparable to those in other T–B–NK+ SCID patients with mutations in the *RAG1*, *RAG2*, or *Artemis* genes (Table 1).

IR sensitivity and different DSB repair kinetics. Fibroblasts derived from patient SC2 showed a more than 3-fold increased x-ray sensitivity (based on 10% survival level) compared with WT primary fibroblasts (FN1). The sensitivity was comparable to that of fibroblasts derived from a patient with NBS (NBS1-LBI) and patients with *Artemis* mutations (Figure 1), suggesting that the patient had a DSB repair defect.

Subsequently, the DSB repair defect was studied in more detail by immunofluorescent staining of DSB repair proteins. Upon IR, several proteins redistribute into IR-induced foci (IRIF) in the nucleus that colocalize with DSBs. Consistent with a DSB repair defect, MRE11 and γ-H2AX IRIF showed an aberrant pattern (Figure 2A). WT fibroblasts showed very few MRE11 and γ-H2AX IRIF 8 hours after irradiation with low doses (1 or 2 Gy), and the number of foci-positive cells and the number of foci per nucleus gradually increased with increasing dose (up to 12 Gy). In patient SC2 fibroblasts, clear MRE11 foci were already observed after irradiation with 1 or 2 Gy, and the individual foci increased in number and appeared much smaller at higher doses of IR, resulting in a "grainy" staining pattern of small foci (Figure 2A). At various time points after x-irradiation, the number of γ-H2AX IRIF per cell was determined in patient SC2 fibroblasts as well as in the LIG4 mutant fibroblasts 180BR and 411BR. As compared with FN1 control cells, SC2 cells showed a slower disappearance of γ-H2AX IRIF per cell, which was even significantly slower than in 180BR and 411BR cells (Figure 2B). This indicates that DSB repair is delayed, probably because of a defect in an NHEJ gene. Slow DSB repair was also demonstrated by pulsed field gel electrophoresis after irradiation with 50 Gy (data not shown). Although patient SC2 fibroblasts had different γ-H2AX IRIF kinetics and delayed DSB repair, there was no evidence for impaired intra–S-phase checkpoint function (see Supplemental Figure 1; supplemental material available online with this article; doi:10.1172/JCI26121DS1) (31).

Block in BM precursor B cell differentiation due to a V(D)J recombination defect. A BM sample from the patient was analyzed by 4-color flow cytometry. Within the lymphocyte gate the percentage of CD22+ (CD36–) precursor B cells was largely comparable to the percentages found in RAG- and Artemis-deficient SCID patients (Table 1). However, the percentage of mature SmIgM+SmIgD+ CD22+ B cells was higher in patient SC2 than in the other T–B–NK+ SCID patients.

Precursor B cells were further subdivided into pro-B, pre-B-I, pre-B-II, and immature B cells. In healthy children, pro-B and pre-B-I cells constituted only 20–25% of the total number of precursor B cells (Figure 3). *RAG* and *Artemis*-deficient SCID patients had a complete block before the CyIgμ+ pre-B-II cell stage due to the V(D)J recombination defect. In patient SC2 the pro-B and pre-B-I

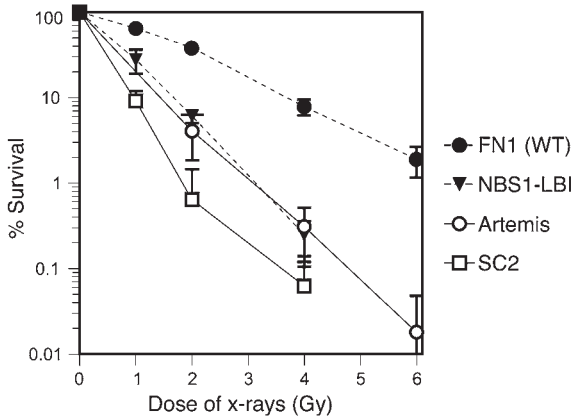

Figure 1
Clonogenic survival assay of fibroblasts after IR. Fibroblasts from patient SC2, the Artemis-deficient SCID patient (Artemis-1), and the NBS1-LBI cell line with an NBS1 mutation were radiosensitive. WT FN1 fibroblasts were used as normal control. Each survival curve represents the mean of at least 3 independent experiments. Error bars represent SEM.

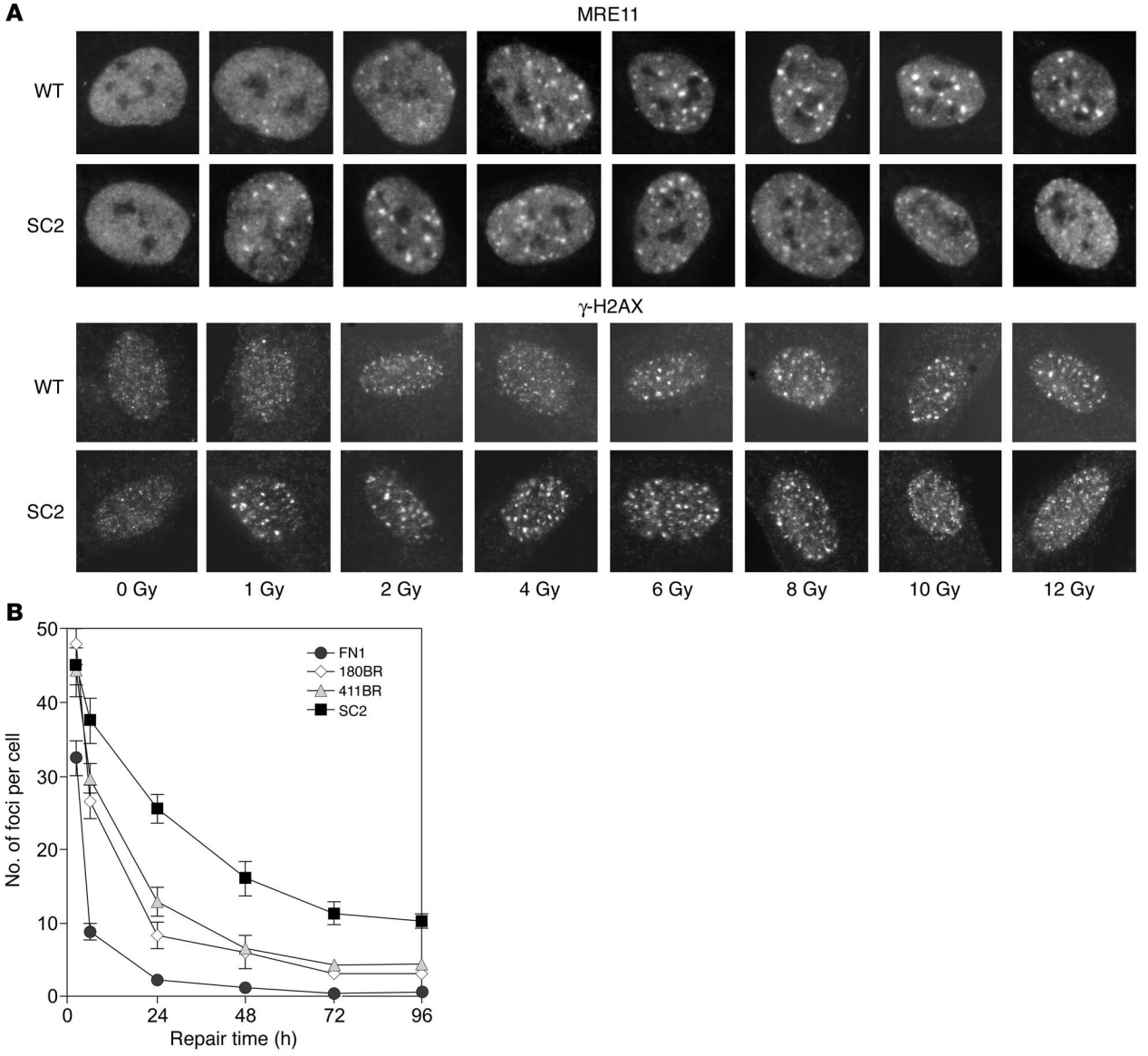

Figure 2
IRIF formation in patient SC2 fibroblasts. (**A**) WT primary human fibroblasts and patient SC2 primary fibroblasts were untreated or γ irradiated with increasing doses (1, 2, 4, 6, 8, 10, and 12 Gy) and fixed after an incubation period of 8 hours followed by immunostaining with the MRE11 or γ-H2AX antibodies. (**B**) Kinetics of loss of γ-H2AX foci in fibroblasts derived from patient SC2 and the LIG4-defective patients 180BR (a radiosensitive leukemia patient) and 411BR (a patient with the LIG4 syndrome), and WT FN1 cells, following x-ray irradiation (1 Gy). The number of foci per nucleus was determined in 40 cells at the indicated times after irradiation.

cells constituted approximately 80% of the precursor B cells, implying that there is an incomplete block in precursor B cell differentiation before the cytoplasmic Igμ$^+$ pre-B-II cell stage (Figure 3).

The incomplete block in B cell differentiation in BM and the presence of very low levels of mature B lymphocytes in peripheral blood were suggestive of a partial but severe V(D)J recombination defect. Therefore the "residual" V(D)J recombination activity was studied by analysis of the D_H-J_H rearrangements in DNA derived from BM mononuclear cells. The D_H-J_H junctions showed remarkably large deletions at the 3′ ends of the D_H segments as well as at the 5′ ends of the J_H gene segments (Table 2). In 2 of the 3 sequences without N nucleotides, microhomology of 1 nucleotide was found. In the remaining sequences, the use of microhomology could not be determined because of the presence of N nucleotides. The nucleotide deletions were much more extensive (3- to 4-fold) than in BM mononuclear cells of a healthy age-matched control. N nucleotides were present, but in lower numbers than in healthy controls. Large stretches of palindromic (P) nucleotides that are found in Artemis-deficient SCID patients were not present in patient SC2 (32) (our unpublished observations).

Insertions or deletions of nucleotides at signal joints are very uncommon. However, none of the 17 IntronRSS–κ-deleting element (IntronRSS-Kde) signal joints in patient SC2 had a precise joint (Table 3). Sequence analysis showed extensive deletions in

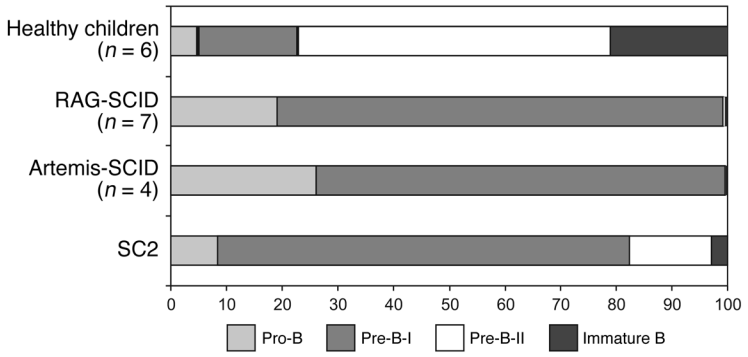

Figure 3
Flow cytometric analysis of BM precursor B cell compartment. Composition of the BM precursor B cell compartment in the patient, healthy controls ($n = 6$), RAG-deficient SCID patients ($n = 7$), Artemis-deficient patients ($n = 4$), and patient SC2. RAG-deficient and Artemis-deficient SCID patients showed a complete block before the CyIgμ-positive pre-B-II cell stage, whereas patient SC2 showed an incomplete block, with approximately 20% pre-B-II and immature B cells.

almost all junctions (average of 13 nucleotides deleted per junction). In 1 junction, no deletion was found, but a 10-nucleotide insertion was found. In addition, 14 of the 17 signal joints displayed signs of repair via microhomology, involving 1 (7 of 14), 2 (1 of 14), or 6 nucleotides (6 of 14).

Complete shift toward microhomology-directed joining of DNA ends. As V(D)J recombination and repair of DSB caused by IR require proper end joining, we studied the circularization of a linear substrate in patient SC2 fibroblasts. Circularization of this DNA substrate can be accomplished by direct joining or microhomology-directed joining of DNA ends (Figure 4A). Mutations in components of DNA-PK or the LIG4/XRCC4 complex cause a dramatic increase in the use of microhomology-directed end joining of a linear substrate in fibroblasts (33). The healthy control as well as the Artemis-deficient fibroblasts (Artemis-1) showed approximately 50% microhomology use (Figure 4B). However, the SC2 cells showed a complete shift toward microhomology-directed joining, as the LIG4 mutant 180BR cells did.

Analysis of genes involved in V(D)J recombination and NHEJ. Sequencing did not show a mutation in *RAG1*, *RAG2*, or *Artemis*. In order to investigate whether proteins involved in NHEJ were normally expressed, Western blot analysis of protein extracts of primary fibroblasts was performed. Similar protein expression levels of XRCC4, KU70, KU80, and DNA-PKcs were found compared with those in the control cells (data not shown), and sequencing of *XRCC4*, *KU70*, or *KU80* did not show mutations. Because of its size, the *DNA-PKcs* gene was not sequenced, but polymorphic markers around this gene showed the same heterozygous genotype in the patient and in one healthy sibling, which rendered a defect in this region unlikely (data not shown). Furthermore, an in vitro DNA-PK assay was performed, which showed that DNA-PK enzyme activity was similar in extracts from patient SC2 and in *Artemis*-deficient cells (Supplemental Figure 2A). DNA-PKcs autophosphorylation after IR was also normal as determined by immunofluorescent staining using a phosphorylation-specific antiserum (Supplemental Figure 2B), suggesting that DNA-PK expression and function are not affected in patient SC2.

Western blot analysis of LIG4 protein expression showed a strong reduction of the approximately 100-kDa band in patient SC2, consistent with reduction of LIG4 protein expression to an undetectable level (Figure 5A). However, the LIG4 antibody recognized several nonspecific products. Therefore, we confirmed the identity of the missing band on Western blot by performing immunoprecipitation of the LIG4/XRCC4 complex using an XRCC4 antibody prior to Western blot analysis. In this case, LIG4 protein could not be precipitated from patient SC2 (Figure 5B), showing that LIG4 expression in patient SC2 is indeed below the detection limit.

Analysis of polymorphic markers around the *LIG4* gene showed that the patient was homozygous for this region whereas both parents and both healthy siblings were heterozygous for it. Sequencing analysis of the *LIG4* gene showed the presence of a homozygous deletion of 3 nucleotides, CAA, at nucleotide posi-

Table 2
Sequences of D_H-J_H junctions derived from BM mononuclear cells of patient SC2 and healthy donors

Patient SC2

D_H segment	3′ deletion	N nucleotides	5′ deletion	J_H segment
D_H2–21	0	G	–7	J_H4
D_H5–24	–13	–	–20	J_H6
D_H2–2	–2	G	–20	J_H4
D_H2–15	–9	CTGT	–15	J_H5
D_H3–9	–12	C	–2	J_H2
D_H2–15	–14	CG	–8	J_H4
D_H4–11	–16	–	–19	J_H4^A
D_H4–17	–5	GCCT	–14	J_H5
D_H4–23	–12	–	–29	$J_H^{A,B}$
D_H5–12	–2	GGG	–9	J_H2
D_H5–24	–62	GGA	–32	J_H^B
D_H5–24	–9	TCGGACAC	–19	J_H4
D_H5–12	–2	CGGTGACA	–14	J_H4
Average	–12.2 ± 15.9	2.8	–16.0 ± 8.5	

Healthy controls

D_H segment	3′ deletion	N nucleotides	5′ deletion	J_H segment
D_H3–10	–4	ACCTAACAGAAAGA	–5	J_H6
D_H2–2	–6	CCCCTTC	–6	J_H5
D_H2–21	–3	AT	–5	J_H5
D_H2–2	–3	C	0	J_H5
D_H3–22	–5	TAAC	–6	J_H4
D_H5–18	–6	CAACA	–7	J_H4
D_H2–21	–5	GAAAGCCCT	–4	J_H6
D_H5–18	–1	TGG	–5	J_H5
D_H2–15	–3	C	0	J_H5
D_H4–17	–3	CCCC	–11	J_H6
D_H4–11	0	ACTCGAAGACCC	–2	J_H6
D_H5–12	0	TAT	–9	J_H4
D_H5–12	–2	TGA	–9	J_H4
D_H5–12	–2	CCCTATTACCATT	–5	J_H6
D_H5–24	–4	AGCT	–21	J_H6
Average	–3.1 ± 1.9	5.7	–6.3 ± 5.1	

[A]Microhomology of 1 nucleotide. [B]J_H could not be assigned because of the size of the deletion; all J_H gene segments are identical in this region.

Table 3
Sequences of signal joints derived from BM mononuclear cells of patient SC2

	Signal joints[A]	Deletions	Insertions
Control[B]	ACGGGCAGCAGGTTGGCAGCGCA**CACTGTG CACAGTG**ATACAAATAATGCCACTAAGGGA	0	
6[C]	ACGGGCAGCAGGTTGGCAGCGCACACTGTG -------ATACAAATAATGCCACTAAGGGA	7	
3	ACGGGCAGCAGGTTGGCAGCGCACA----- ----------GGGA	31	
1	ACGGGCAGCAGGTTGGCAGCGCACACTG-- -------ATACAAATAATGCCACTAAGGGA	9	
4	ACGGGCAGCAGGTTGGCAGCGCACA----- --------TACAAATAATGCCACTAAGGGA	13	
1	ACGGGCAGCAGGTTGGCAGCGCACA----- ----------AGGGA	30	T
1	ACGGGCAGCAGGTTGGCAGCGCACACTGT- CACAGTGATACAAATAATGCCACTAAGGGA	1	
1	ACGGGCAGCAGGTTGGCAGCGCACACTGTG CACAGTGATACAAATAATGCCACTAAGGGA	0	CACACACACA

[A]Bolded nucleotides indicate the heptamer sequences of the RSS in the control sequence; underlined nucleotides are involved in repair via microhomology. [B]Sequence of a precise signal joint formed after the rearrangement of IntronRSS-Kde as found in controls. [C]Number of clones found with the indicated type of signal joint.

tion 5,333–5,335 (AF479264, National Center for Biotechnology Information [NCBI] Nucleotide database; http://www.ncbi.nlm.nih.gov/entrez/query.fcgi?db=Nucleotide). *LIG4* transcripts were present. Deletion of these 3 nucleotides resulted in deletion of glutamine Q433 in the protein (NP_996820, NCBI Nucleotide database). The absence of detectable levels of LIG4 protein suggests that this mutation severely affects protein stability.

Complementation with WT LIG4. In the end-joining assay of the linearized substrate, patient SC2 fibroblasts showed a complete shift toward microhomology-directed joining, whereas control cells showed equal usage of microhomology-directed and direct joining. Therefore, we chose this assay for complementation. The end-joining assay was repeated with and without cotransfection of a WT LIG4 expression construct. We expected only partial complementation, because the linearized substrate and the WT LIG4 expression construct are transfected at the same moment and therefore circularization of the linearized substrate will take place in the absence of LIG4 during the first few hours after transfection, until WT LIG4 is expressed.

Analysis of the joints in SC2 cells showed 5% direct joining, which was increased to 35% upon expression of WT LIG4, compared with 45% and 48% in WT fibroblasts without and with additional LIG4 expression, respectively (average of 2 experiments; Figure 6). This indicates that WT LIG4 can complement the joining defect in patient SC2, confirming that the repair defect in patient SC2 is caused by the LIG4 mutation.

Discussion

We present a new type of radiosensitive $T^-B^-NK^+$ SCID without a defect in *Artemis*, but with a mutation in the *LIG4* gene. To date, *LIG4* mutations have been described only in 4 patients with a designated LIG4 syndrome (19, 29), which is associated with chromosomal instability, pancytopenia, and developmental and growth delay; in 1 radiosensitive leukemia patient; and in a sixth patient with acute T cell leukemia and NBS-like facial abnormalities (30). The clinical presentation of our patient differed from RS-SCID caused by an *Artemis* defect with respect to the age of onset. The LIG4-deficient RS-SCID patient developed normally in the first year of life, but in the second year of life she began to suffer from severe infections of the respiratory tract, candidiasis in the diaper region, and subsequent chronic diarrhea and fever, whereas in Artemis-deficient RS-SCID patients the symptoms already develop in the first 6 months of life. Compared with patients with the LIG4 syndrome, the LIG4-deficient RS-SCID patient had a severe immunodeficiency. Her T cells were strongly reduced in number and had a strongly diminished proliferative response, characteristic of SCID. Secondary to this immunodeficiency, she developed failure to thrive. Microcephaly and neurological abnormalities as seen in the LIG4 syndrome were not present in our patient. Recently, the impact of LIG4 defect on class switch recombination was studied in 2 patients with the LIG4 syndrome (34). Similar analyses could not be performed in our patient because of the virtually complete absence of B cells, which illustrates the difference between the two *LIG4*-deficient disease entities.

The *LIG4* mutation in the LIG4-deficient RS-SCID patient concerned a homozygous deletion of 3 nucleotides resulting in deletion of glutamine at position 433. Q433 is located between 2 conserved stretches in the catalytic domain of LIG4 (35). The deletion resulted in undetectable levels of LIG4 protein, most probably due to instability of the LIG4 protein. The *LIG4* mutations that

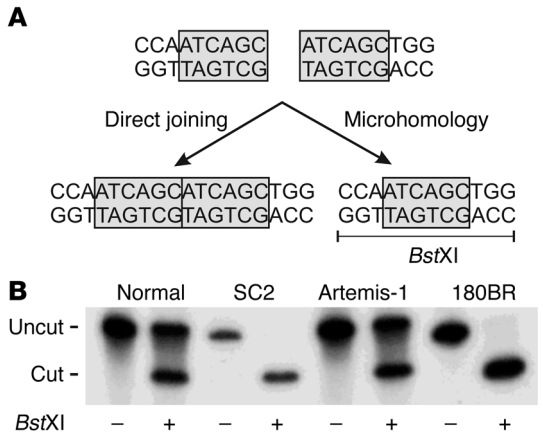

Figure 4
DNA end joining. (**A**) A linear substrate with homologous ends (ATCAGC) can be rejoined via direct end joining or via microhomology-directed end joining. Joining via microhomology results in the generation of a *Bst*XI restriction site ($CCAN_6TGG$). (**B**) Analysis of joining products in WT (Normal), SC2, Artemis (Artemis-1), and LIG4 mutant (180BR) cells. Junctions were PCR amplified, and PCR products were digested with *Bst*XI, as indicated.

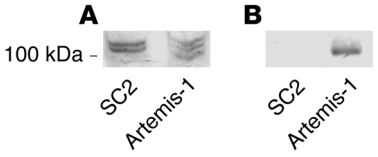

Figure 5
Analysis of LIG4 protein expression. (**A**) Western blot analysis of LIG4 protein expression showed absence of an approximately 100-kDa band in patient SC2. Artemis-1 was used as positive control. The position of the 100-kDa band of the molecular weight marker is indicated on the left. (**B**) After immunoprecipitation of the LIG4/XRCC4 complex with the XRCC4 antibody, no LIG4 protein was detectable in patient SC2.

have been reported previously resulted in normal levels of protein with impaired function. These *LIG4* mutations were regarded as hypomorphic, because *LIG4*-deficient mice have defective neurogenesis due to neuronal apoptosis, resulting in embryonic lethality (24, 25). The delQ433 mutation in our patient appeared to have a strong impact on V(D)J recombination, thus resulting in $T^-B^-NK^+$ SCID, but did not result in microcephaly or neurological abnormalities; this suggests some residual LIG4 activity from very low levels of protein (below our detection limit).

The delQ433 mutation resulted in a strongly reduced efficiency of DSB repair, which was illustrated by disturbed kinetics of IRIF formation of MRE11 and γ-H2AX and pulsed field gel electrophoresis. The delQ433 mutation also affected the ligation phase of V(D)J recombination, resulting in an incomplete but severe block in precursor B cell differentiation at the transition of the pre-B-I to the pre-B-II stage and strongly reduced numbers of B cells in peripheral blood.

Analysis of Ig gene junctional regions gives insight into the type of V(D)J recombination defect and can be used as a diagnostic tool for $T^-B^-NK^+$ SCID patients or other patients with a suspected defect in NHEJ. Mutations in the *Artemis* gene result in large stretches of P nucleotides (9, 32, 36) (our unpublished observations). These long stretches of P nucleotides are explained by aberrant hairpin opening, which is normally mediated by DNA-PK–activated Artemis. Based on mouse data, it is known that DNA-PKcs mutations also give rise to large stretches of P nucleotides (9, 32, 36). *KU70/KU80*–deficient mice show absence of N nucleotides in the coding junctions, because TdT requires binding to KU70/KU80 to exert its function. In addition, microhomology use was frequently found in the coding joints of *KU70/KU80*–deficient mice (37). In the low levels of residual D_H-J_H junctions and signal joints of our LIG4-deficient RS-SCID patient, microhomology use was also found, but N nucleotides were readily detected, albeit at low levels. Most remarkably, the junctions in the patient showed extensive nucleotide deletions, on average 12–16 nucleotides. Apparently the LIG4 deficiency causes a severe delay in the ligation of the gene segments (if they are ligated at all) allowing prolonged exonuclease activity.

Large deletions can affect the V(D)J recombination process in 4 ways. First, the entire D_H gene segment and its 5′ RSS can be deleted, making the next V_H-to-D_H/J_H recombination step impossible. Second, extensive deletions resulting in loss of the entire J_H gene segment and the downstream splice site will lead to inability to splice the V(D)J exon to the exon encoding the constant region. Third, extensive deletions of more than 6 nucleotides at the 3′ side of VH gene segments will delete the cysteine codon, which codes for the intrachain disulfide bond that is responsible for the V_H protein folding. Finally, large deletions will result in a substantial decrease of the size of the complementarity-determining region 3 (CDR3), which can affect the Ig repertoire and antigen recognition. Although BM-derived junctional regions were not studied in other LIG4 patients, V(D)J recombination was studied in LIG4-deficient cells 180BR, 411BRneo, and LB2304 using recombination substrates, which also gave rise to junctions with extensive deletions (29, 38).

A second characteristic of the coding junctions was a reduced number of N nucleotides at the junctions. The reduction of N nucleotide addition might be explained by less efficient introduction of these nucleotides by TdT, which would suggest a direct effect of LIG4 on TdT activity. However, we assume that this phenomenon is caused by prolonged exonuclease activity, due to slower DSB repair kinetics and decreased DNA end protection by the LIG4/XRCC4 complex.

Finally, both coding and signal joints displayed signs of microhomology use. Two of the 3 coding joints without N nucleotides displayed 1-nucleotide microhomologies. In the other sequences, microhomology use could not be determined because of the presence of N nucleotides that obscure microhomology. However, the vast majority of signal joints, which do not have N regions, clearly displayed microhomology-directed end joining. These results are in line with the complete shift toward use of microhomology-directed end joining of a linear substrate in patient SC2 as well as in 180BR fibroblasts. A similar shift toward microhomology-directed joining was observed after creation of a blunt DSB by transposon Tn5 excision in *XRCC4*-deficient cells (39).

This study shows that *LIG4* mutations can give rise not only to the LIG4 syndrome, characterized by pancytopenia and neurological defects, but also to RS-SCID without neurological defects and pancytopenia (except for lymphopenia). Since our LIG4-deficient RS-SCID patient died at the age of 2 years, the child may have been too young to develop the LIG4 syndrome, although microcephaly was certainly not observed. However, we think that the different clinical presentations are most probably due to the different types of mutations resulting in normal levels of low-activity protein (as found in LIG4 syndrome) versus an undetectable level of LIG4 protein (as found in RS-SCID). Apparently, low levels of LIG4 protein are sufficient for cell survival, but V(D)J recombination clearly requires higher LIG4 protein levels. It is possible that this difference in behavior between neuronal and lymphoid cells is caused by a different mechanism of apoptosis induction in the 2 cell types. The relatively high level of LIG4 protein that is required in developing lymphoid cells is in line with our recent observation that *LIG4* transcripts are the only transcripts of members of the NHEJ machinery that are differentially expressed dur-

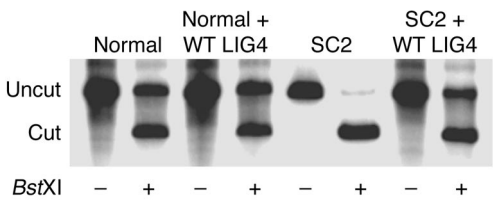

Figure 6
Complementation of end-joining defect with the WT LIG4. Analysis of joining products of the linear substrate with homologous ends (Figure 4A) in WT and SC2 patients with and without cotransfection of a WT LIG4 expression construct. Junctions were PCR amplified, and PCR products were digested with *Bst*XI, as indicated.

ing precursor B cell differentiation, with increased expression in the pre-B-I and small pre-B-II stages, during which Ig heavy and Ig light chain rearrangements, respectively, take place (40). Further evidence for our hypothesis on the different effects of *LIG4* mutations will have to come from identification of additional patients with *LIG4* mutations and/or mouse models mimicking these patients' mutations.

Methods

Case report. SCID patient SC2 was a firstborn girl of healthy, consanguineous Turkish parents without a family history of specific diseases. The child reached normal developmental milestones during the first year of life and did not show mental retardation at admission. Her growth chart showed –1 SD for length, +0.5 SD for weight, and –0.5 SD for head circumference. However, in her second year of life she developed recurrent severe infections of the respiratory tract and candidiasis in the diaper region. Subsequently, she suffered from chronic diarrhea, fever, and failure to thrive. Her growth showed a decline for weight and length (to –2 SD and –3 SD, respectively). At 18 months she was admitted to our hospital under the clinical suspicion of a severe immunodeficiency.

Laboratory results revealed a hemoglobin level of 6.2 mmol/l, a leukopenia of 4.2×10^9 per liter, and low Ig levels: IgG 0.94 g/l, IgA 0.12 g/l, and IgM 0.50 g/l. T/B/NK cell analysis of the peripheral blood showed strongly reduced numbers of B cells and T cells, but normal NK cell counts, fitting with the diagnosis of $T^-B^-NK^+$ SCID (Table 1). The few remaining T cells were autologous and had a strongly reduced proliferative response. After stimulation with PHA and anti-CD3, their proliferation (based on ^{3}H-TdR incorporation) was reduced 100-fold to 200 cpm (normal value >17,500 cpm) and 20 cpm (normal value >1,500 cpm), respectively. The lymphocyte proliferation assay was repeated 1 month later, giving fully comparable results. Extensive microbiological investigations did not reveal a specific pathogen except candidiasis of skin and mouth. Upon treatment with antibiotics and Ig substitution, the clinical condition of the child improved.

Because of the SCID diagnosis, a BM transplantation was planned, but initially no HLA-identical donor was found. However, at time of the SCID diagnosis, the mother was 26 weeks pregnant, and the birth of the second child, who could possibly serve as a donor, was awaited. The newborn child appeared to be HLA identical and healthy, so a cord blood stem cell procedure was initiated. Conditioning before stem cell infusion was given according to the prevailing European protocols, consisting of busulfan 2 daily doses 25 mg (days –9 to –6) and cyclophosphamide 1 daily dose 500 mg (days –5 to –2). Unfortunately, the clinical condition of the patient deteriorated during the conditioning period. She developed severe nausea and vomiting, more than is usually seen with this protocol, and edema. She was suspected of vascular leakage syndrome, possibly due to veno-occlusive disease. Despite treatment, she further deteriorated clinically and biochemically and died eventually from a bradycardia and respiratory arrest.

Approval for this study was obtained from the Medisch Ethische Commissie, Erasmus Medical Center. Cell samples were obtained with informed consent according to the local guidelines.

Cell lines and tissue culture. Primary and hTert immortalized fibroblasts from skin biopsies were used from the SC2 patient described in this paper and from the Artemis-deficient patient Artemis-1 (16). Other fibroblast cell cultures used in this study were 180BR and 411BR with a mutation in *LIG4* (kindly provided by P. Jeggo, Genome Damage and Stability Centre, University of Sussex, Falmer, Brighton, United Kingdom) (28, 29), AT2RO with a mutation in *ATM*, NBS1-LBI with a mutation in *NBS1* (41), and the control cell cultures FN1 and C5RO from skin biopsies of healthy volunteers. All cell lines were cultured in Ham's F10 medium (BioWhittaker), supplemented with 15% FCS, penicillin (100 U/ml), and streptomycin (100 μg/ml).

Clonogenic survival assay and immunocytochemistry of fibroblasts after irradiation. Primary fibroblasts of the patient were used in a clonogenic survival assay that was performed as described before (16).

For postirradiation immunophenotyping, fibroblasts were grown on glass coverslips and irradiated using a ^{137}Cs source (~1 Gy/min) with various doses. At various time points from 0.5 to 24 hours, they were fixed with 2% paraformaldehyde. Cells were washed with BSA and glycine in PBS and permeabilized with 0.1% Triton X-100 in PBS. The following antibodies were applied: anti-MRE11 (42), anti-RAD51 (rabbit polyclonal antibody, our own stock) (43), and anti–γ-H2AX (rabbit polyclonal antibody; Upstate). After 90 minutes, the cells were washed as described above, and Alexa 594–conjugated goat anti-rabbit (Invitrogen Corp.) was applied. Cells were incubated for 60 minutes and subsequently washed with 0.1% Triton X-100 in PBS and regular PBS. Coverslips were put on object glasses covered with VECTASHIELD containing DAPI (Vector Laboratories) and sealed. Analysis of foci was performed using a Leica DMRBE fluorescent microscope (Leica Microsystems Inc.) connected to a Hamamatsu dual-mode cooled charge-coupled device camera C4480 (Hamamatsu Photonics). To visualize the fluorescence pattern, the 31000 (DAPI) and 31004 (Alexa 594) filtersets were used.

To examine the kinetics of loss of γ-H2AX foci, cells were kept confluent for 1 week prior to x-irradiation. Cells were irradiated with 1 Gy of x-rays (dose rate of ~2.8 Gy/min; 200 kV, 4 mA, 0.78 mm Al), and, 2, 24, 48, 72, and 96 hours after treatment, the cells on the slides were fixed with 2% paraformaldehyde. After permeabilization with 0.2% Triton X-100 in PBS, and blocking with PBS$^+$ (20 mM glycine 0.5% wt/vol BSA in PBS), the cells were incubated with monoclonal mouse anti–γ-H2AX (Upstate) and subsequently with Alexa 488–conjugated goat anti-mouse IgG (Invitrogen Corp.). Cell nuclei were stained with DAPI (Sigma-Aldrich). The number of γ-H2AX foci per cell was counted under a Zeiss Axioplan fluorescence microscope and 40 cells per cell line were scored at each time point.

Flow cytometric immunophenotyping of BM leukocytes and analysis of coding and signal joints. For flow cytometric analysis of BM, 50-μl aliquots of BM mononuclear cells (10×10^6 per milliliter) were used in each of the 12 four-color labelings (16, 44).

DNA was isolated from BM mononuclear cells of patient SC2 and healthy donors. For analysis of coding joints, D_H-J_H gene rearrangements were amplified by PCR. In addition, signal joints formed after the rearrangement of IntronRSS to the Ig Kde were amplified (45). In each 50-μl reaction, 250 ng of DNA, 5 pmol 5′ and 3′ primers, and 1 U of AmpliTaq Gold polymerase (Applied Biosystems) were used (46). PCR products derived from D_H-J_H gene rearrangements and IntronRSS-Kde signal joints were cloned in pGEM-Teasy prior to sequencing with BigDye Terminator mix (Applied Biosystems) using 3.3–6 pmol sequencing primers. Sequencing was performed on an ABI 377 or ABI 3100 fluorescent sequencer (Applied Biosystems).

Analysis of NHEJ via transfection of linearized DNA substrates in an end-joining assay and Western blot analysis of proteins involved in DNA DSB repair. Linearized pDVG94 containing a microhomology at the ends (ATCAGC sequence) was transfected into primary fibroblasts. The newly formed junctions were PCR amplified, and the relative use of the microhomology was assayed by digestion with the restriction enzyme BstXI (33).

For Western blot analysis, whole-cell extracts of the fibroblasts were prepared, separated by SDS-PAGE, and transferred to a nitrocellulose membrane. The proteins of interest were visualized using antibodies against the following proteins: MRE11 (rabbit polyclonal antibody) (42), RAD50 (mouse mAb, 13B3; GeneTex Inc.), ATM (rabbit polyclonal antibody, AB91; Abcam Ltd.), XRCC4 (rabbit polyclonal antibody, NIH14; gift from M. Modesti, Erasmus Medical Center), KU70 (goat polyclonal antibody, C-19; Santa Cruz Biotechnology Inc.), KU80 (goat polyclonal antibody, C-20; Santa Cruz Bio-

technology Inc.), DNA-PKcs (rabbit polyclonal antibody produced against amino acids 356–570), and LIG4 (rabbit polyclonal antibody; Serotec). Alkaline phosphatase–conjugated goat anti-rabbit, goat anti-mouse, or sheep anti-goat IgGs were used as secondary antibodies (BioSource International).

Immunoprecipitation of LIG4/XRCC4 complex. One hundred micrograms of whole-cell extracts (47) of patient SC2 and Artemis-SCID fibroblasts were incubated overnight at 4°C with an anti–human XRCC4 antibody (mouse anti–human XRCC4; Abcam Ltd.) and protein G-Sepharose beads (protein G Sepharose 4 Fast Flow; Amersham Biosciences). The protein G beads were washed several times with PBS and boiled for 5 minutes in protein sample buffer, and the supernatant of the boiled samples was separated by SDS-PAGE and transferred to a nitrocellulose membrane for detection of LIG4 protein. The LIG4 protein was visualized with rabbit anti–human LIG4 (Serotec) as described above.

Complementation assay of LIG4 defect. The end-joining assay was used as complementation assay by cotransfection of 1 μg of the WT eGFP-LIG4 expression construct (kindly provided by M. Modesti) in addition to the linearized pDVG94 substrate in patient SC2 fibroblasts and in C5RO fibroblasts.

PCR/RT-PCR sequencing analysis, and analysis of polymorphic markers. PCR analysis of *RAG1/RAG2* and *Artemis* was performed as described before (16, 44). PCR analysis of *LIG4* was performed using 100 ng of DNA isolated from granulocytes in 100-μl reactions containing 30 pmol of 5′ and 3′ primers, 35 nmol dNTP, and 7.5 U Expand polymerase mixture (Roche Diagnostics Corp.) with supplied buffer (Roche Diagnostics Corp.). The long-range–PCR conditions were 2 minutes at 94°C, followed by 38 cycles of 15 seconds at 94°C, 30 seconds at 57°C, and 4 minutes at 68°C using 10 seconds of autoextension from cycle 21 onward. RT-PCR analysis of *KU70*, *KU80*, and *XRCC4* was performed with 5 pmol 5′ and 3′ primers, 0.25 μg cDNA prepared from mRNA isolated from fibroblasts using random hexamers and SuperScript reverse transcriptase (Invitrogen Corp.) (48), and 1 U of AmpliTaq Gold polymerase (Applied Biosystems) or 7.5 U Expand polymerase mixture. PCR/RT-PCR products were purified using QIAquick PCR purification kit (QIAGEN). Sequencing was performed on an ABI 377 or ABI 3100 fluorescent sequencer (Applied Biosystems).

Four polymorphic markers flanking *DNA-PKcs* (D8S1771, D8S505, D8S285, D8S260) and *LIG4* (D13S158, D13S173, D13S1265, D13S285) were amplified by PCR followed by electrophoretic analysis of PCR products.

Acknowledgments

We thank P.A. Jeggo for providing us with the 180BR and 411BR human fibroblasts and for critical reading of the manuscript. We thank D. Chen (Lawrence Berkeley National Laboratory, Berkeley, California, USA) for the antisera against T2609-phosphorylated DNA-PKcs and M. Modesti for the eGFP-LIG4 expression construct. We thank E. Weterings for the purified DNA-PK protein and J.G. Noordzij and G. Breedveld for technical assistance. This work was supported by grants from the Dutch Cancer Society (KWF; grant EMCR 2002-2734), the Dutch Organization for Scientific Research (NWO; grant AGIKO 920-03-089), and the European Union (RISC-RAD).

Received for publication June 30, 2005, and accepted in revised form October 18, 2005.

Address correspondence to: Dik C. van Gent, Department of Cell Biology and Genetics, Erasmus Medical Center, University Medical Center Rotterdam, Dokter Molewaterplein 50, 3015 GE Rotterdam, The Netherlands. Phone: 31-10-4087932; Fax: 31-10-4089468; E-mail: d.vangent@erasmusmc.nl.

Mirjam van der Burg and Lieneke R. van Veelen contributed equally to this work.

1. Schatz, D.G. 2004. V(D)J recombination. *Immunol. Rev.* **200**:5–11.
2. Gellert, M. 2002. V(D)J recombination: RAG proteins, repair factors, and regulation. *Annu. Rev. Biochem.* **71**:101–132.
3. McBlane, J.F., et al. 1995. Cleavage at a V(D)J recombination signal requires only RAG1 and RAG2 proteins and occurs in two steps. *Cell.* **83**:387–395.
4. Van Gent, D.C., Ramsden, D.A., and Gellert, M. 1996. The RAG1 and RAG2 proteins establish the 12/23 rule in V(D)J recombination. *Cell.* **85**:107–113.
5. Lees-Miller, S.P., and Meek, K. 2003. Repair of DNA double strand breaks by non-homologous end joining. *Biochimie.* **85**:1161–1173.
6. Grawunder, U., and Harfst, E. 2001. How to make ends meet in V(D)J recombination. *Curr. Opin. Immunol.* **13**:186–194.
7. Benedict, C.L., Gilfillan, S., Thai, T.H., and Kearney, J.F. 2000. Terminal deoxynucleotidyl transferase and repertoire development. *Immunol. Rev.* **175**:150–157.
8. Van Gent, D.C., Hoeijmakers, J.H., and Kanaar, R. 2001. Chromosomal stability and the DNA double-stranded break connection. *Nat. Rev. Genet.* **2**:196–206.
9. Smith, G.C., and Jackson, S.P. 1999. The DNA-dependent protein kinase. *Genes Dev.* **13**:916–934.
10. Burma, S., and Chen, D.J. 2004. Role of DNA-PK in the cellular response to DNA double-strand breaks. *DNA Repair (Amst.)* **3**:909–918.
11. Moshous, D., et al. 2001. Artemis, a novel DNA double-strand break repair/V(D)J recombination protein, is mutated in human severe combined immune deficiency. *Cell.* **105**:177–186.
12. Ma, Y., Pannicke, U., Schwarz, K., and Lieber, M.R. 2002. Hairpin opening and overhang processing by an Artemis/DNA-dependent protein kinase complex in nonhomologous end joining and V(D)J recombination. *Cell.* **108**:781–794.
13. Lieber, M.R., Ma, Y., Pannicke, U., and Schwarz, K. 2003. Mechanism and regulation of human non-homologous DNA end-joining. *Nat. Rev. Mol. Cell Biol.* **4**:712–720.
14. Schwarz, K., et al. 1996. RAG mutations in human B cell-negative SCID. *Science.* **274**:97–99.
15. Nicolas, N., et al. 1998. A human severe combined immunodeficiency (SCID) condition with increased sensitivity to ionizing radiations and impaired V(D)J rearrangements defines a new DNA recombination/repair deficiency. *J. Exp. Med.* **188**:627–634.
16. Noordzij, J.G., et al. 2003. Radiosensitive SCID patients with Artemis gene mutations show a complete B-cell differentiation arrest at the pre-B-cell receptor checkpoint in bone marrow. *Blood.* **101**:1446–1452.
17. Li, L., et al. 2002. A founder mutation in Artemis, an SNM1-like protein, causes SCID in Athabascan-speaking Native Americans. *J. Immunol.* **168**:6323–6329.
18. Kobayashi, N., et al. 2003. Novel Artemis gene mutations of radiosensitive severe combined immunodeficiency in Japanese families. *Hum. Genet.* **112**:348–352.
19. O'Driscoll, M., Gennery, A.R., Seidel, J., Concannon, P., and Jeggo, P.A. 2004. An overview of three new disorders associated with genetic instability: LIG4 syndrome, RS-SCID and ATR-Seckel syndrome. *DNA Repair (Amst.)* **3**:1227–1235.
20. Moshous, D., et al. 2003. Partial T and B lymphocyte immunodeficiency and predisposition to lymphoma in patients with hypomorphic mutations in Artemis. *J. Clin. Invest.* **111**:381–387. doi:10.1172/JCI200316774.
21. Dai, Y., et al. 2003. Nonhomologous end joining and V(D)J recombination require an additional factor. *Proc. Natl. Acad. Sci. U. S. A.* **100**:2462–2467.
22. Frank, K.M., et al. 1998. Late embryonic lethality and impaired V(D)J recombination in mice lacking DNA ligase IV. *Nature.* **396**:173–177.
23. Gao, Y., et al. 1998. A critical role for DNA end-joining proteins in both lymphogenesis and neurogenesis. *Cell.* **95**:891–902.
24. Barnes, D.E., Stamp, G., Rosewell, I., Denzel, A., and Lindahl, T. 1998. Targeted disruption of the gene encoding DNA ligase IV leads to lethality in embryonic mice. *Curr. Biol.* **8**:1395–1398.
25. Frank, K.M., et al. 2000. DNA ligase IV deficiency in mice leads to defective neurogenesis and embryonic lethality via the p53 pathway. *Mol. Cell.* **5**:993–1002.
26. Gao, Y., et al. 2000. Interplay of p53 and DNA-repair protein XRCC4 in tumorigenesis, genomic stability and development. *Nature.* **404**:897–900.
27. Lee, Y., Barnes, D.E., Lindahl, T., and McKinnon, P.J. 2000. Defective neurogenesis resulting from DNA ligase IV deficiency requires Atm. *Genes Dev.* **14**:2576–2580.
28. Riballo, E., et al. 1999. Identification of a defect in DNA ligase IV in a radiosensitive leukaemia patient. *Curr. Biol.* **9**:699–702.
29. O'Driscoll, M., et al. 2001. DNA ligase IV mutations identified in patients exhibiting developmental delay and immunodeficiency. *Mol. Cell.* **8**:1175–1185.
30. Ben-Omran, T.I., Cerosaletti, K., Concannon, P., Weitzman, S., and Nezarati, M.M. 2005. A patient with mutations in DNA ligase IV: clinical features and overlap with Nijmegen breakage syndrome.

Am. J. Med. Genet. A. **137**:283–287.
31. Stewart, G.S., et al. 1999. The DNA double-strand break repair gene hMRE11 is mutated in individuals with an ataxia-telangiectasia-like disorder. *Cell.* **99**:577–587.
32. Rooney, S., et al. 2003. Defective DNA repair and increased genomic instability in Artemis-deficient murine cells. *J. Exp. Med.* **197**:553–565.
33. Verkaik, N.S., et al. 2002. Different types of V(D)J recombination and end-joining defects in DNA double-strand break repair mutant mammalian cells. *Eur. J. Immunol.* **32**:701–709.
34. Pan-Hammarstrom, Q., et al. 2005. Impact of DNA ligase IV on nonhomologous end joining pathways during class switch recombination in human cells. *J. Exp. Med.* **201**:189–194.
35. Doherty, A.J., and Suh, S.W. 2000. Structural and mechanistic conservation in DNA ligases. *Nucleic Acids Res.* **28**:4051–4058.
36. Lewis, S.M. 1994. P nucleotide insertions and the resolution of hairpin DNA structures in mammalian cells. *Proc. Natl. Acad. Sci. U. S. A.* **91**:1332–1336.
37. Bogue, M.A., Wang, C., Zhu, C., and Roth, D.B. 1997. V(D)J recombination in Ku86-deficient mice: distinct effects on coding, signal, and hybrid joint formation. *Immunity.* **7**:37–47.
38. Riballo, E., et al. 2001. Cellular and biochemical impact of a mutation in DNA ligase IV conferring clinical radiosensitivity. *J. Biol. Chem.* **276**:31124–31132.
39. van Heemst, D., Brugmans, L., Verkaik, N.S., and van Gent, D.C. 2004. End-joining of blunt DNA double-strand breaks in mammalian fibroblasts is precise and requires DNA-PK and XRCC4. *DNA Repair (Amst.)* **3**:43–50.
40. Van Zelm, M.C., et al. 2005. Ig gene rearrangement steps are initiated in early human precursor B cell subsets and correlate with specific transcription factor expression. *J. Immunol.* **175**:5912–5922.
41. Kraakman-van der Zwet, M., et al. 1999. Immortalization and characterization of Nijmegen Breakage syndrome fibroblasts. *Mutat. Res.* **434**:17–27.
42. de Jager, M., et al. 2001. DNA-binding and strand-annealing activities of human Mre11: implications for its roles in DNA double-strand break repair pathways. *Nucleic Acids Res.* **29**:1317–1325.
43. Essers, J., et al. 2002. Nuclear dynamics of RAD52 group homologous recombination proteins in response to DNA damage. *EMBO J.* **21**:2030–2037.
44. Noordzij, J.G., et al. 2002. The immunophenotypic and immunogenotypic B-cell differentiation arrest in bone marrow of RAG deficient SCID patients corresponds to residual recombination activities of mutated RAG proteins. *Blood.* **100**:2145–2152.
45. Langerak, A.W., et al. 2004. Unraveling the consecutive recombination events in the human IGK locus. *J. Immunol.* **173**:3878–3888.
46. Szczepanski, T., et al. 1999. Ig heavy chain gene rearrangements in T-cell acute lymphoblastic leukemia exhibit predominant DH6-19 and DH7-27 gene usage, can result in complete V-D-J rearrangements, and are rare in T-cell receptor alpha beta lineage. *Blood.* **93**:4079–4085.
47. Manley, J.L., Fire, A., Samuels, M., and Sharp, P.A. 1983. In vitro transcription: whole-cell extract. *Methods Enzymol.* **101**:568–582.
48. Van Dongen, J.J.M., et al. 1999. Standardized RT-PCR analysis of fusion gene transcripts from chromosome aberrations in acute leukemia for detection of minimal residual disease. Report of the BIOMED-1 Concerted Action: investigation of minimal residual disease in acute leukemia. *Leukemia.* **13**:1901–1928.
49. Comans-Bitter, W.M., et al. 1997. Immunophenotyping of blood lymphocytes in childhood. *J. Pediatr.* **130**:388–393.
50. Muller, S.M., et al. 2001. Transplacentally acquired maternal T lymphocytes in severe combined immunodeficiency: a study of 121 patients. *Blood.* **98**:1847–1851.
51. Noordzij, J.G., et al. 2002. Composition of the precursor B-cell compartment in bone marrow from patients with X-linked agammaglobulinemia compared to healthy children. *Pediatr. Res.* **51**:159–168.